Research Report

Hydrogen-rich saline improves memory function in a rat model of amyloid-beta-induced Alzheimer's disease by reduction of oxidative stress

Jian Li[a], Cai Wang[a], John H. Zhang[b], Jian-Mei Cai[c], Yun-Peng Cao[a],*, Xue-Jun Sun[c],*

[a]Department of Neurology, the First Affiliated Hospital of China Medical University, Shengyang 110001, PR China
[b]Department of Neurosurgery, Loma Linda University, California, CA, USA
[c]Department of Diving Medicine, Faculty of Naval Medicine, Second Military Medical University, Shanghai, 200433, PR China

A B S T R A C T

This study is to examine if hydrogen-rich saline reduced amyloid β (Aβ) induced neural inflammation, and learning and memory deficits in a rat model. S-D male rats ($n=84$, 280–330 g) were divided into three groups, sham-operated, Aβ1-42 injected and Aβ1-42 plus hydrogen-rich saline-treated animals. Hydrogen-rich saline (5 ml/kg, i.p., daily) was injected for 14 days after intracerebroventricular injection of Aβ1-42. The levels of MDA, IL-6 and TNF-α were assessed by biochemical and ELISA analysis. Morris Water Maze and open field task were used to assess the memory dysfunction and motor dysfunction, respectively. LTP were used to detect the electrophysiology changes, HNE and GFAP immunohistochemistry were used to assess the oxidative stress and glial cell activation. After Aβ1-42 injection, the levels of MDA, IL-6, and TNF-α were increased in brain tissues and hydrogen-rich saline treatment suppressed MDA, IL-6, and TNF-α concentration. Hydrogen-rich saline treatment improved Morris Water Maze and enhanced LTP in hippocampus blocked by Aβ1-42. Furthermore, hydrogen-rich saline treatment also decreased the immunoreactivity of HNE and GFAP in hippocampus induced by Aβ1-42. In conclusion, hydrogen-rich saline prevented Aβ-induced neuroinflammation and oxidative stress, which may contribute to the improvement of memory dysfunction in this rat model.

© 2010 Elsevier B.V. All rights reserved.

1. Introduction

Alzheimer's disease (AD) is the most common cause of progressive dementia in the elderly population. It has been estimated that about 5% of the population older than 65 years is affected by Alzheimer's disease. There is an enormous medical need for the development of novel therapeutic strategies that target the underlying pathogenic mechanisms in AD. The proposed pathogenic mechanisms for AD generally include loss of cholinergic function, oxidative stress, amyloid cascade, inflammatory mediators, steroid hormone deficiencies, and excitotoxicity (Shah et al., 2008). Among them the

amyloid cascade hypothesis is well accepted which suggesting a central role of Aβ in the pathogenesis. It has been shown that accumulation of β-amyloid (in particular of the Aβ1-42 peptide) in the brain initiates a cascade of events that ultimately leads to neuronal dysfunction, neurodegeneration and dementia (Klafki et al., 2006).

Molecular hydrogen (H_2) is a special free radical scavenger which uniquely reduces hydroxyl radicals (•OH), but not superoxide (O_2–•), hydrogen peroxide (H_2O_2), or nitric oxide (NO•) (Buxton et al., 1998; Ohsawa et al., 2007). There are several recent studies reported that molecular hydrogen reduced oxidative stress and its associated disorders. Molecular hydrogen in the form of gas or H_2-saturated saline reduced the cerebral infarction (Ohsawa et al., 2007) and decreased apoptosis in neonatal hypoxic brain injury in rats (Cai et al., 2008, 2009). Molecular hydrogen dissolved in drinking water similarly attenuated sclerotic lesions (Ohsawa et al., 2008) and prevented cisplatin-induced nephrotoxicity in mice (Nakashima-Kamimura et al., 2009). To date, most of these studies have been focused on the ischemic and reperfusion injury and the potential effect of hydrogen in AD has not been tested. We hypothesize that hydrogen may attenuate AD by reduction of oxidative stress. We tested this hypothesis by using an intracerebroventricular (i.c.v.) injection of Aβ rat model. The role of MDA, TNF-α, IL-6, LTP, HNE and GFAP in Aβ-induced early impairment of learning and memory were assessed by giving hydrogen-rich saline.

2. Results

2.1. Hydrogen saline improved learning and memory

The escape latency was recorded at 8 days after Aβ1-42 injection. In training trials, the escape latency time on the last training day (the fifth day) was 10.64±8.62 s in sham group, 30.10±20.93 s in Aβ1-42 plus physiological saline group, and 18.14±16.16 s in Aβ1-42 plus hydrogen-rich saline group. Among them, the escape latency time is significantly different between sham and Aβ1-42 plus physiological saline groups ($p<0.05$), but not between sham and Aβ1-42 plus hydrogen-rich saline groups ($p=0.093$). In probe trials, animals in hydrogen-rich saline group spent more time on the right quadrant for searching the platform when compared with Aβ1-42 plus physiological saline group ($p=0.026$) (Figs. 1A–E), suggesting hydrogen-rich saline improved spatial recognition and memory that had declined by Aβ1-42.

No alterations of the swimming speed ($F=1.73$; $p=0.18$) in the Morris Water Maze (Fig. 1F), or the total squares crossed ($F=0.81$; $p=0.45$) and rearing behavior ($F=0.62$; $p=0.54$) in the open field arena (Figs. 1G–H) were observed, indicating no motor deficits in this animal model.

2.2. Hydrogen saline enhanced LTP in hippocampus in vivo

In sham group rats, 200 Hz conditioning stimulation induced a robust and stable LTP of the EPSP amplitude compared to pre-HFS baseline (177±5% of baseline at 1 h post-HFS). The LTP produced in the Aβ1-42 (2.2 nmol) group (127±6%) following

HFS was significantly depressed compared with sham group ($p=0.000$), and hydrogen-rich saline (148±8%) attenuated this inhibition significantly ($p=0.000$) (Fig. 2).

2.3. Hydrogen saline suppressed lipid peroxidation

Lipid peroxidation was assessed by detecting brain tissue MDA level and hippocampus immunostaining using anti-HNE antibody. The content of MDA in Aβ1-42 plus physiological saline group (6.71±1.08) was significantly increased compared to the sham group (4.21±0.78) ($p=0.000$). Hydrogen-rich saline administration suppressed the production of MDA (5.64±0.76) when compared with that in the Aβ1-42 plus physiological saline group ($p=0.018$) (Fig. 3A). On the other hand, HNE immunoreactivity was rarely observed in the dentate gyrus of hippocampus in the sham group 14 days after operation. The number of stained cells per $0.01\,mm^2$ in dentate gyrus of hippocampus increased significantly in Aβ injection rats compared with sham group ($p=0.000$). In the hydrogen-rich saline rats, the number of HNE-positive cells were significantly decreased compared with the Aβ group ($p=0.011$) (Figs. 3B–C).

2.4. Effects of hydrogen saline on inflammatory responses

ELISA detection showed that the levels of TNF-α and IL-6 in brain tissue were markedly increased by 2.23-fold and 2.10-fold in Aβ1-42 plus saline-treated group, and 2.06-fold and 2.04-fold in Aβ1-42 plus hydrogen-rich saline-treated group, when compared with sham-operated controls. Hydrogen-rich saline reduced the elevation of IL-6 and TNF-α in the brain tissues (Figs. 4A–B).

2.5. Hydrogen saline inhibited the Aβ1-42 induced astrocytes activation

The astrocyte reaction was visualized by means of the immunoreactivity for glial fibrillar acidic protein (GFAP), a specific marker of astrocytes. Aβ1-42 resulted in infiltration of astrocytes in hippocampal CA1 and dentate gyrus, as well as transformation of astrocytes from a resting to an activated state, highlighted by phenotypic changes characterized by long, thick branching and distended cell body. Hydrogen-rich saline significantly inhibited the Aβ1-42 induced astrocytic reaction in hippocampal CA1 and dentate gyrus (Figs. 5A–B).

3. Discussion

In the present study, we analyzed the mechanisms of action of hydrogen saline in a rat model of i.c.v. injection of Aβ1-42. A single i.c.v. injection of a nanomolar dose of Aβ1-42 effectively impaired learning and memory behavior in rats. Furthermore, this behavioral abnormality was accompanied by increases in hippocampal GFAP/HNE immunoreactivity and high level of inflammation cytokine in brain tissue, which all have been reported existed in clinical AD patients. The major findings of the present study were that hydrogen saline significantly improved learning memory and LTP, suppressed the early accumulation of lipid peroxidation products, and eliminated
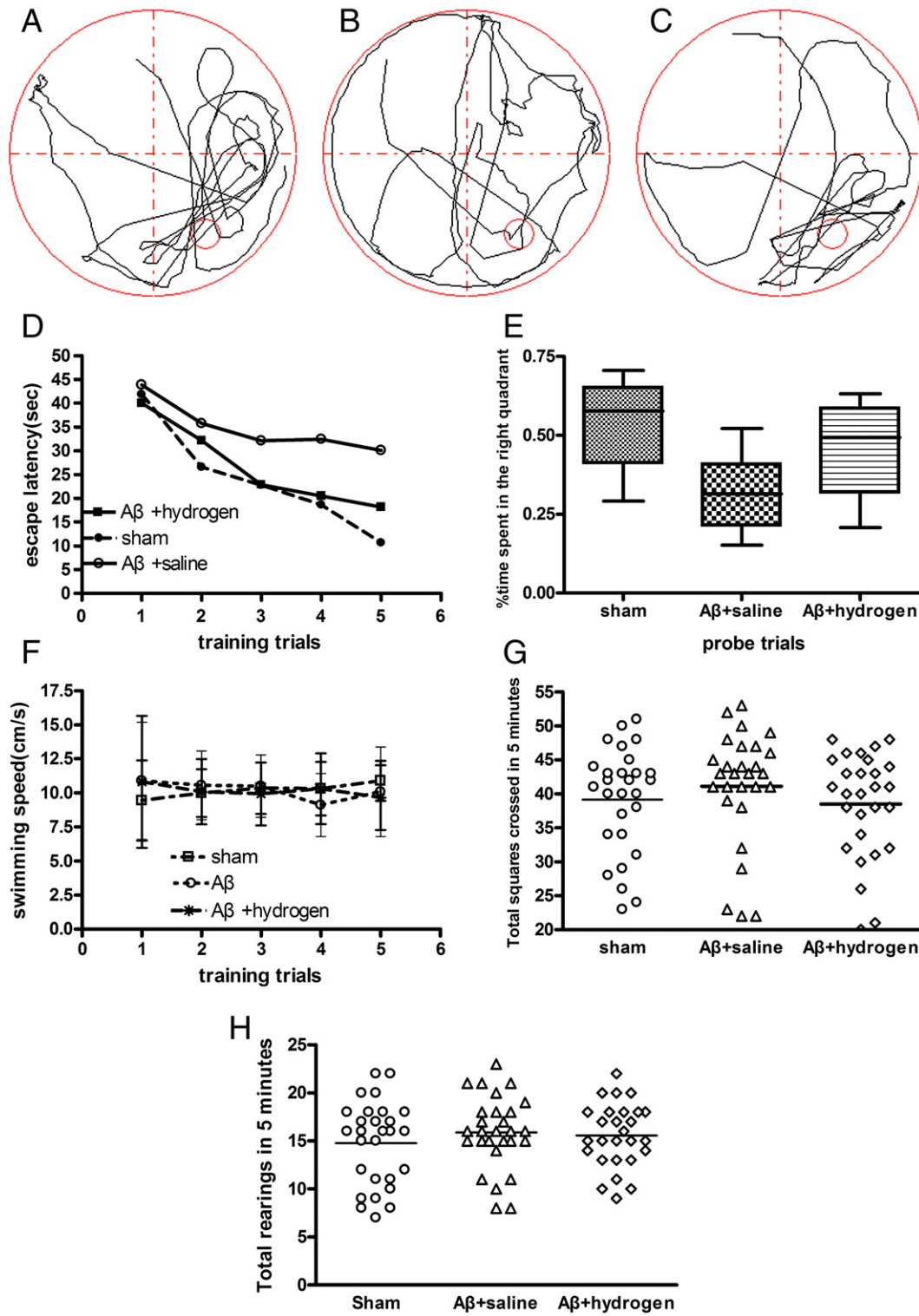
Fig. 1 – Representative swim traces of each group in probe trials: (A) sham, (B) Aβ + saline, (C) Aβ + hydrogen, (D) escape latencies in training trials, and (E) percent goal quadrant dwell time in the probe trials. On the sixth day of initial training, rats were allowed to swim for 60 s in the maze without the escape platform, and the time spent in each quadrant was recorded. Hydrogen-rich saline treatment rats spent more time in the target quadrant compared to the saline treatment. (F) Swimming speed in training trials, (G) squares crossed and (H) rearings in 5 min in open field test showed no different in motor function in each group.

the sequential inflammatory responses. Taken together, results from the present study illustrate the validity of this animal model for at least some aspects of Alzheimer's disease.

The training and the probe trials showed cognitive and memory functional decline in this animal model indicating this model resembles Alzheimer's like disorders. Using this
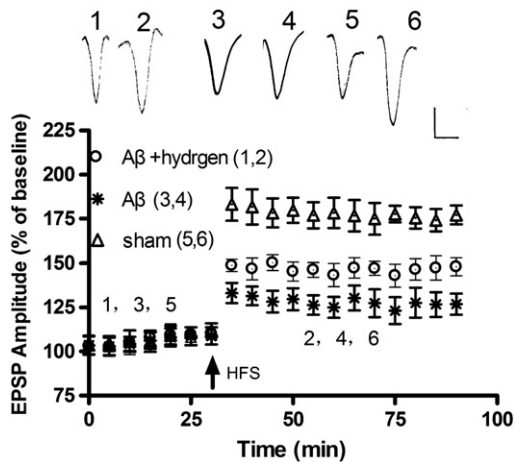
Fig. 2 – Hydrogen-rich saline attenuated the depression of LTP induced by Aβ1-42. The LTP produced in the Aβ1-42 (2.2 nmol) group following HFS was significantly depressed compared with sham group (*p* = 0.000), and hydrogen-rich saline attenuated this inhibition significantly (*p* = 0.000).Each point is an average of 3 responses and were obtained at 5 minute intervals. The arrows indicate the time at tetanization. Insets: representative example of EPSP traces pre-HFS and post-HFS in each group. Scale bar indicates 1mv/5 ms.

animal model, we observed that hydrogen-rich saline improved learning and memory functions probably by its anti-neuroinflammation and anti-oxidative stress actions. Long-term potentiation (LTP) is an enhanced synaptic transmission observed in synapses that have previously been stimulated. It can be considered to be a mechanism that supports learning and memory functions, was shown to be severely impaired in old Tg2576 mice (Chapman et al., 1999). Aβ peptide oligomers rapidly and significantly block LTP (Walsh et al., 2002). The correlation between LTP and performance on the spatial learning and memory task is of great interest. Although the correlation does not show a direct link between LTP and behavior, it nonetheless demonstrates that treatments producing a deficit in the former also produce deficits in the latter, which was verified in our study.

A pathologic hallmark of AD is the formation of senile plaques. β-Amyloid peptide (Aβ), a 39–43 amino acid peptide, is a major component of these plaques. Strong evidence has shown that free radicals and oxidative stress induced by Aβ play an important role in neurodegeneration of AD (Smith et al., 2006; Guidi et al., 2006; Ohta and Ohsawa, 2006). Free radicals which produce lipid peroxidation, protein peroxidation, DNA peroxidation and oxidative stress are the central elements of age-related diseases (Calabrese et al., 2006; Zhu et al., 2006; Loh et al., 2006; Koliatsos et al., 2006). Clinical and basic science evidences indicate that oxidative stress is associated with aging and AD and markers of oxidative stress have been shown to precede pathological lesions in AD, including senile plaques and neurofibrillary tangles (Castellani et al., 2001; Nunomura et al., 1999, 2001; Sayre et al., 1997). Antioxidants thus have potentials to blunt the cognitive decline in AD or to slow disease progression (Jama et al.,

1996; Perrig et al., 1997; Rottkamp et al., 2000). Therefore, in this study we measured the levels of the malondialdehyde (MDA) which is the product of lipid membrane oxidation and represents the production of the reactive oxygen species (ROS). Its content responses to speed and intensity of lipid peroxidation, it indirectly responds to the damage degree of free radical. Furthermore, we detected 4-hydroxynonenal (HNE) production in hippocampus which is produced when superoxide peroxidates arachidonic acid in the lipid bilayer, and is a well-known oxidative stress marker (Hayashi et al., 2003). Analysis of AD brains demonstrates an increase in free HNE in amygdala, hippocampus, and parahippocampal gyrus of the AD brain compared with age-matched controls (Markesbery and Lovell, 1998). A significant elevation of free HNE in ventricular CSF and serum provides a potential biomarker for AD (Lovell et al., 1997). HNE is elevated in neurons treated with Aβ1-42 (Lauderback et al., 2001). HNE inhibits plasma membrane transporters, disrupts the assembly of microtubules and inhibits mitochondrial function (Picklo et al., 2001). HNE has also been shown to inhibit choline acetytransferase, the enzyme responsible for the synthesis of acetylcholine (Butterfield and Lauderback, 2002). Increased levels of MDA have been identified early in the course of the disease in the vulnerable superior and middle temporal gyri of the Alzheimer brain and not in other regions. MDA levels have even been found increased in these regions in patients with minimal cognitive impairment, a condition that often precedes AD (Keller et al., 2005). It has been reported that Aβ fragments are neurotoxic to hippocampal and cortical neurons either in vitro or in vivo (Chen et al., 1996; Nakamura et al., 2001; Shen et al., 2002). Aβ peptide produces hydrogen peroxide through metal ion reduction, with concomitant release of thiobarbituric acidreactive substances, a process probably mediated by formation of hydroxyl radicals and the subsequent oxidative reactions (Mecocci et al., 1994; Huang et al., 1999a,b). In the present study, we observed that hydrogen saline treatment actually decreased oxidative neuronal stress by demonstrating the change in HNE immunoreactivity in hippocampus. Hydrogen-rich saline reduced MDA content in this Aβ1-42 induced Alzheimer's like-disease animal model.

In addition, the inflammatory cytopathology may be a secondary response to the early accumulation of Aβ in the brain. Common neuroinflammatory events include activation and proliferation of microglia and astrocytes, activation of nuclear transcription factor kappa β, upregulation of inflammatory cytokines such as tumor necrosis factor α and interleukin 1β, release of prostaglandin E_2 under the enzymatic control of cyclooxygenase-2, and release of reactive oxygen and nitrogen species. The innate immune response that occurs in the brain leads to the accumulation of inflammatory mediators such as TNF-α, IL-1, IL-6, free radicals, complement components and microglia activation (Weiner and Selkoe, 2002). These neuroinflammation makers are typically observed in association with AD neuropathology. TNF-α is a multifunctional cytokine that triggers a wide range of cellular responses. In the CNS, TNF-α disrupts learning and memory and regulates neuronal death. TNF-α has also been shown to participate in Aβ-induced inhibition of LTP, a form of synaptic plasticity closely associated with learning and memory. In the present study the levels of TNF-α and IL-6
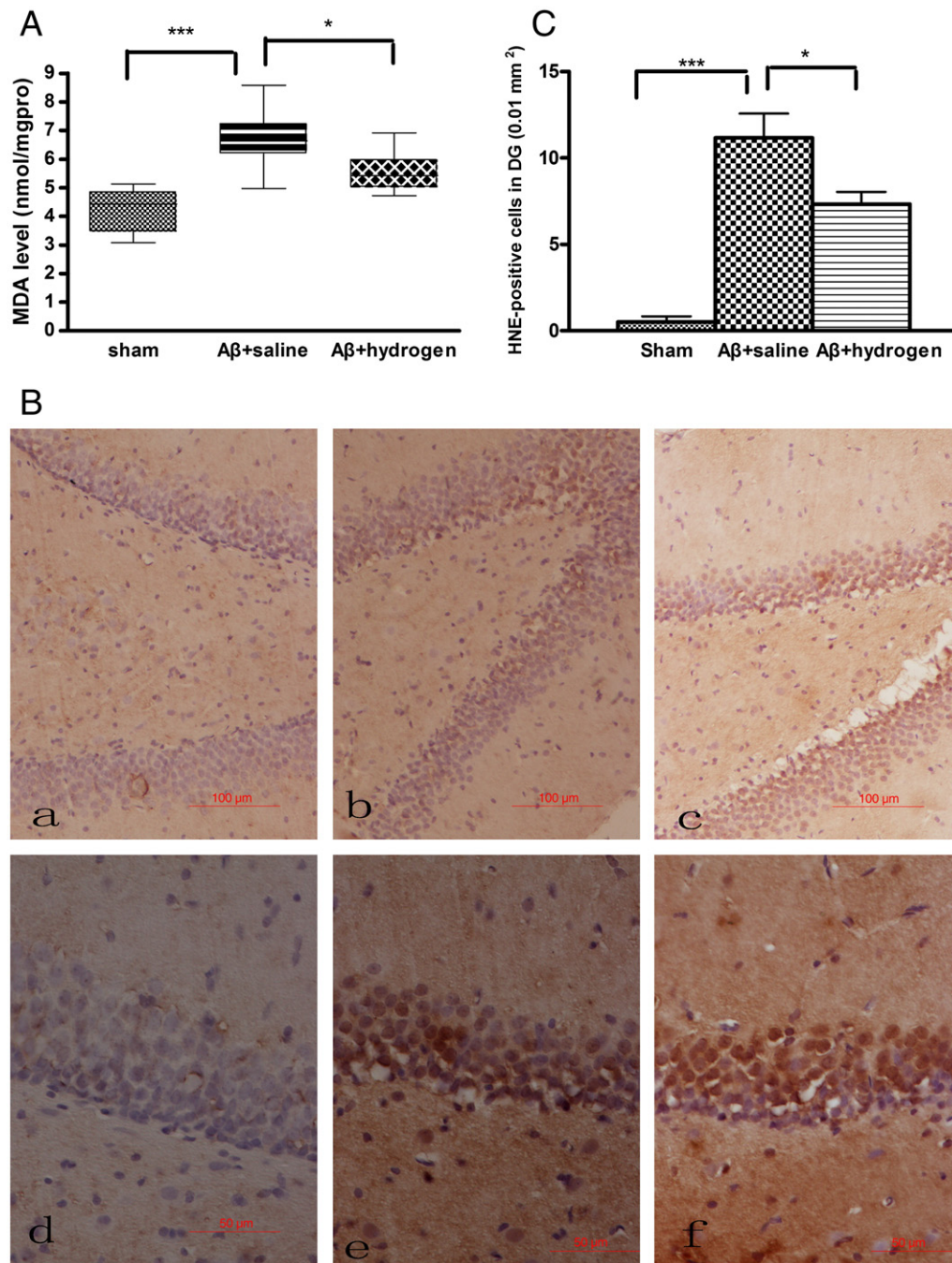
Fig. 3 – (A) The MDA level in brain tissues. Aβ1-42 enhanced MDA levels and hydrogen-rich saline reduced MDA. (B) Immunohistochemical examples for 4-hydroxynonenal (HNE) in the dentate gyrus of hippocampus. In contrast to almost no immunoreactivity in the sham control, many neurons became strongly stained in the amyloid-beta-treated brains in dentate gyrus of hippocampus 14 days after operation. Treatment with hydrogen-rich saline reduced the degree of staining than the amyloid group. (a, d sham group; b, e hydrogen group; and c, f Aβ group. scale bar: a–c 100 μm, d–f 50 μm). (C) Number of HNE-positive cells in the hippocampus dentate gyrus in each group. Quantitative analysis revealed that hydrogen-rich-saline-treated groups showed statistically significant reduction of stained cells. Values are expressed as the number of positive cells per 0.01 mm^2 (mean ± SEM). $n = 6$ each group. $^*p < 0.05$; $^{***}p < 0.001$.

increased significantly in this Aβ1-42 rat model, which was decreased by hydrogen-rich saline treatment.

Reactive gliosis is a response of astrocytes to a variety of results that is characterized by hypertrophy of the cell bodies and processes and an increase in the expression of GFAP. AD is clinically characterized by progressive dementia. Neuropathologically, the hippocampus is one of the first and most severely damaged structures in AD. Furthermore, prominent inflammatory responses take place in AD that involves the activation of microglia and astrocytes (Nagele et al., 2004;
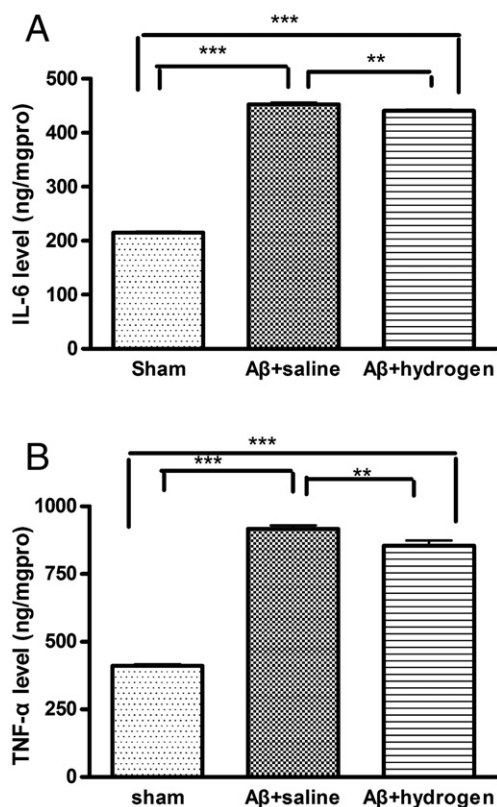
Fig. 4 – The IL-6 (A) and TNF-α (B) levels in brain tissues. Aβ1-42 increased IL-6 and TNF-α and hydrogen-rich saline prevented the elevation of IL-6 and TNf-α. *$p<0.05$, **$p<0.01$, ***$p<0.001$.

Meda et al., 2001). Classic astrogliosis is known to occur extensively in the senile AD cortex and CA1 region. Karin Boekhoorn (Boekhoorn et al., 2006) found a robust astrogliosis in the SGZ in young AD patients. In our study, cells staining for GFAP were found in the dentate gyrus molecular layer and hilar region, as well as in the molecular layer of CA1 after amyloid injection. Less GFAP-positive cells were showed in hydrogen-rich saline rats. The experiments have demonstrated that the hydrogen-rich saline can reduce the astrocytes activation induced by amyloid-beta.

The relationship between oxidative stress and inflammation is complex. Reactive oxygen species may release TNF-α by activating NF-κB (Castranova, 2004; Min et al., 2003), and anti-oxidative stress may decrease the level of TNF-α in cells (Barrett et al., 1999). In addition, reactive oxygen species enhance the expression of adhering and chemotactic molecules, resulting in neutrophils, mononuclear cells, and lymphatic cells adhesion to the endothelium. Local chemotaxis, accumulation and infiltration of those white blood cells subsequently aggravate inflammatory responses (Ichikawa et al., 1997; Jiang et al., 2005; Kokura et al., 2002). Anti-oxidative treatments inhibited the expression of adhering molecules and therefore relieved the inflammatory responses (Jiang et al., 2004). Therefore, we speculate that hydrogen-rich saline improved learning and memory ability in this Aβ1-42 animal model by anti-neuroinflammation via anti-oxidative stress action.

Taking together, hydrogen-rich saline improved the cognitive and memory functions in this Aβ1-42 Alzheimer's like-disorder animal model. The therapeutic effect of hydrogen-rich saline may be mediated by its anti-oxidative stress which may contribute to neuroinflammation. One of the advantages of hydrogen-rich saline is its ability to cross the blood–brain barrier and therefore has potentials in neurological disorders including Alzheimer's disease.

## 4. Experimental procedures

4.1. Animals and drug treatment

Male Sprague–Dawley rats (Experimental Animal Center of China Medical University, Shengyang, China), maintained at an ambient temperature of 22–24 °C under a 12 h:12 h light: dark cycle, were used in this experiment. Animals were divided into three groups ($n=28$ each group): (1) sham-operated plus physiological saline treatment; (2) Aβ1-42 (2.2 nmol/10 μl) i.c.v. (intracerebroventricularly) injection plus physiological saline treatment; and (3) Aβ1-42 (2.2 nmol/10 μl) i.c.v. injection plus hydrogen-rich saline treatment (5 ml/kg, i.p., daily). Amyloid-β1-42 (Sigma-Aldrich, Beijing, China) was suspended at a concentration of 1 μg/μl. To obtain the aggregated form of Aβ1-42, the peptide solution was placed in an incubator at 37 °C for 72 h.

4.2. Hydrogen-rich saline production

Hydrogen was dissolved in physiological saline for 6 h under high pressure (0.4 MPa) to a supersaturated level using hydrogen-rich saline-producing apparatus produced by the Diving Medicine Department of the 2nd Military Medical University in Shanghai China. The saturated hydrogen-rich saline was stored under atmospheric pressure at 4–8 °C in an aluminum bag with no dead volume. Hydrogen-rich saline was sterilized by gamma radiation. Hydrogen-rich saline was freshly prepared every week, which ensured that a concentration of 0.6 mmol/l was maintained. Gas chromatography was used to confirm the content of hydrogen in saline by the method described by Ohsawa et al. (2007).

4.3. Surgery

All experimental procedures were carried out in accordance with the guidelines of the Animal Care and Use Committee of the China Medical University. The rats weighing 280–330 g were anesthetized with chloral hydrate (300 mg/kg) intraperitoneally and placed in a stereotaxic apparatus (Stoelting, USA) with the incisor bar set at 3.3 mm below the interaural line. Small burr holes were made in the parietal bone to allow the insertion of the injection cannula. Briefly, Aβ1-42 (1 nmol) (Sigma-Aldrich, Beijing, China) was injected bilaterally into the lateral ventricles through a stainless steel cannula (antero-posterior: –0.8 mm relative to bregma, medial/lateral: –1.4 mm relative to bregma, and dorsal/ventral: –4.0 mm below dura) by means of a Hamilton microsyringe. Body temperature was maintained at 37 °C. The injection lasted 5 min and the needle with the syringe was left in place for 2 min after the injection
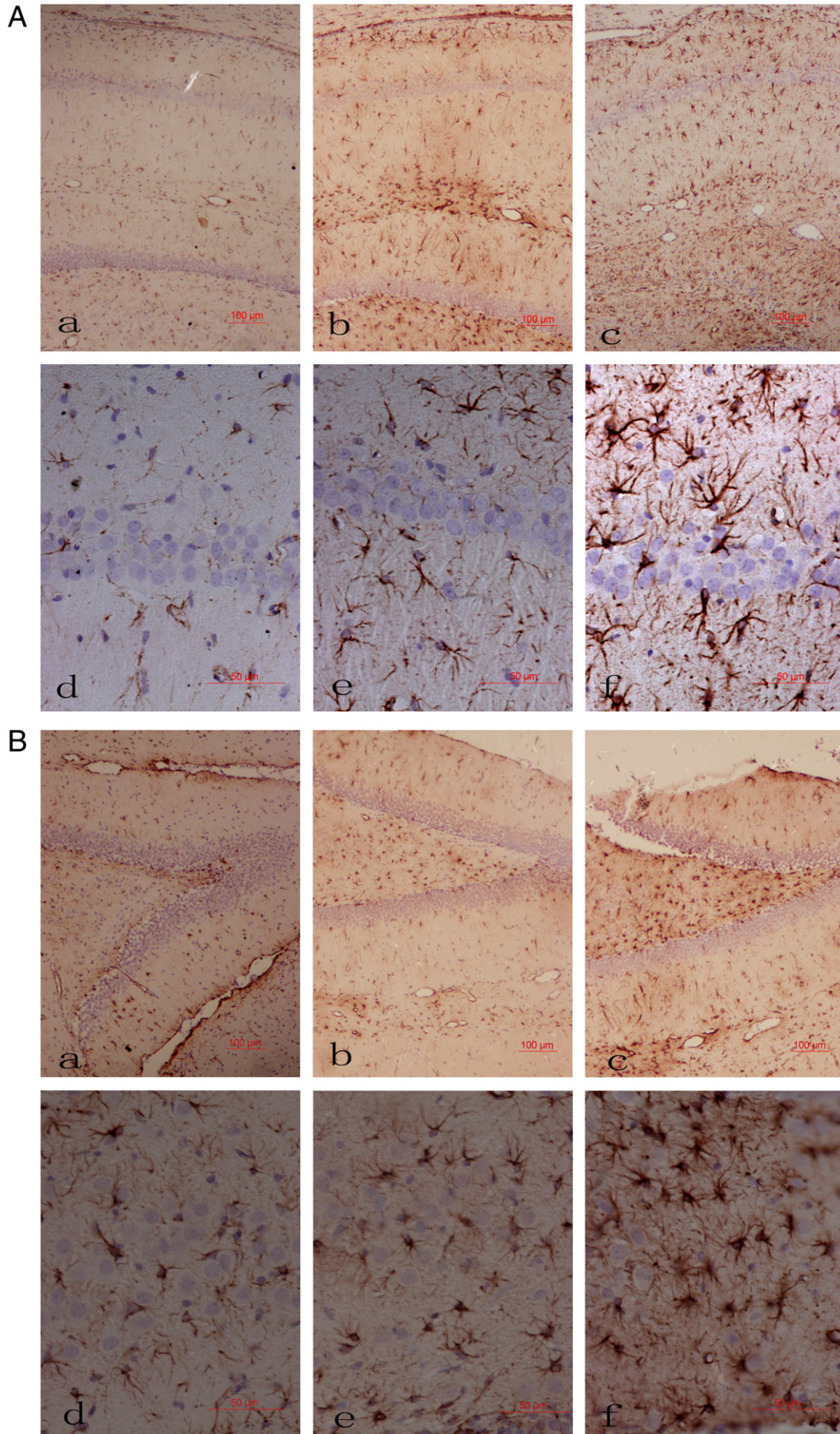
for the completion of drug infusion. After Aβ1-42 injection the rats were administrated with hydrogen-rich saline or physiological saline through an intraperitoneal method (5 ml/kg, i.p., daily) for 2 weeks.

4.4. Morris Water Maze (MWM) and open field task

The experimental apparatus (Chinese Academy of Science, China) consisted of circular water tank (diameter, 130 cm; height, 50 cm) containing water at 23 ± 2 °C. The target platform (10×10 cm) was submerged 1 cm below the water surface and placed at the midpoint of one quadrant. The platform was fixed at the position, equidistant from the center and the wall of the pool. The pool was placed in a test room containing various prominent visual cues. Rats were subject to a spatial reference memory version of the water maze as described previously (Prediger et al., 2007). The acquisition training session was performed 8 days after Aβ1-42 injection. The animals were left in the tank facing the wall and allowed to swim freely to the escape platform. If an animal did not find the platform within a period of 60 s, it was gently guided to it. The animal was allowed to remain on the platform for 15 s after escaping to it. This procedure was repeated 10 times and the escape latency time was recorded and calculated. The test session was performed 24 h after the training session. The test session consisted of a single probe trial in which the platform was removed from the pool and each rat was allowed to swim for 60 s in the maze. The time spent in the correct quadrant (i.e., where the platform was located on the training session) was recorded, and the percentage of the total time was calculated.

To verify the effects of i.c.v. treatment with Aβ1-42 on locomotor activity, the animals were placed for 5 min in the open field arena after the last MWM test. The apparatus was made of wood covered with impermeable Formica, had a white floor measuring 100×100 cm (divided by black lines into 25 squares of 20×20 cm) and was surrounded by 40-cm high walls. The experiments were conducted in a sound attenuated room. Each rat was placed in the centre of the open field and the numbers of squares crossed and rearings were registered.

4.5. Electrophysiology test

Following the behavioral testing, six rats of each group were tested for hippocampal long term potentiation (LTP). The animals were anesthetized with urethane (20%, 5 ml/kg, i.p.) and stereotaxically implanted with a recording electrode aimed at the granule cell (GC) layer of the dentate gyrus (DG) and a stimulating electrode aimed at the perforant path (PP). The experimental paradigm consisted of first adjusting the stimulating and recording electrodes to produce maximum field responses. A test stimulus (0.25 ms pulse-width) was then selected that would elicit a small population spike (1–2 mV; approximately 1/3 of saturation current). The amplitude

of EPSP was calculated and displayed graphically to ascertain the induction of LTP. A baseline was then obtained by delivering a pulse (0.25 ms pulse-width) to the PP every 30 s for 30 min, and recording the field potentials (average of 3 responses, 1/5 s). Following baseline recordings, brief tetanic stimulation, at an intensity level sufficient to induce a minimum spike, was delivered to the PP (10 pulses, 200 Hz, 5 times, 10 s apart) and the field responses were once again calculated for 10 min. The intensity of the tetanic stimulation was then increased to a level approximately 40% of saturation and the procedure was repeated. Tetanization at this second, higher stimulus intensity was performed to ensure that the responses were not saturated following the first tetanus. The EPSP amplitude was used to measure synaptic efficacy. EPSPs are expressed as a percentage of the mean initial amplitude measured during the last 10 min of the baseline-recording period prior to LTP induction. LTP data recorded between 55 and 60 min post-HFS were analyzed.

4.6. Immunohistochemistry

Fourteen days after injection of Aβ1-42, the rats were perfused transcardially with 4% paraformaldehyde in phosphate buffered saline (PBS). The brains were removed and postfixed for 24 h and were embedded in paraffin wax. Serial coronal sections (5 μm thickness) were cut from various sections of the brain. After the coronal sections were rinsed in PBS 3 times, endogenous peroxidase activity was blocked by incubation with 3% H_2O_2 for 10 min. The sections were incubated with 10% normal goat serum. After the blocking serum was removed, sections were immunostained overnight at 4 °C using a rabbit polyclonal antibody against 4-hydroxy-2-nonenal (HNE; 500:1; Alpha Diagnostic International, USA) to assess lipid peroxidation, a mouse monoclonal antibody against GFAP (GFAP ; 100:1; Beyotime , China) to assess astrocyte activation, then with biotinylated secondary antibody at 37 °C for 20 min. The HNE-positive and GFAP-positive cells were detected using strept-avidinbiotin complex (SABC) and DAB kits (Zhongshan, China). Images were captured with a microscope (Nikon Eclipse 80i) and Digital Sight Camera (DS-5M-L1, Nikon, NY, USA). Control and experimental tissues were placed on the same slide and processed under the same conditions. The settings for image acquisition were identical for control and experimental tissues. In each HNE section, the stained cells were counted in 3 predefined areas (0.01 mm^2; $n=6$ each group) from dentate gyrus of hippocampus. An observer blind to group assignment performed the analysis.

4.7. Malondialdehyde (MDA) assay

Six rats each group were sacrificed at 14 days after Aβ1-42 injection. The left prefrontal cortex were carefully excised and powdered using a motor and pestle on dry ice and immediately stored at –70 °C for determining the content of MDA.

Fig. 5 – Immunostaining of glial fibrillary acidic protein (GFAP) in the hippocampus CA1 (A) and dentate gyrus (DG) (B). (a, d) Very little signal is present in the CA1 and DG area of a sham subject immunostained for GFAP. (c, f) Conversely, many GFAP-positive reactive astrocytes are present in CA1 and DG area of an amyloid-beta subject. (b, e) Hydrogen-rich saline attenuated the activation of astrocytes. a, d Sham group; b, e hydrogen group; and c, f Aβ group. Scale bar represents 100 μm (a–c) and 50 μm (d–f).

MDA content in brain cortex homogenates were determined with chemical method described by the manufacturer's instructions (Nanjing Jiancheng Biochemistry Co., Nanjing, China). Cortex tissue (100 mg, wet wt) was homogenized in 1 ml of 10 mM phosphate buffer (pH 7.4). After centrifugation at 12,000×g for 20 min, the MDA content in supernatant were assessed spectrophotometrically with the corresponding kits (Nanjing Jiancheng Biochemistry Co., Nanjing, China). Lipid peroxidation levels were determined by the thiobarbituric acid (TBA) reaction which measures the color change at 535 nm with spectrometer. TBARS levels were expressed as nmol/mg protein in the brain. The protein content was quantified by Commassie blue assay.

4.8.   TNF-α and IL-6 levels

The specimens of the right brain tissues were used to determine the protein level of TNF-α (tumor necrosis factor-α) and IL-6 (interleukin-6) at 20 h after operation. The homogenates were centrifuged at 3000×g at 4 °C for 15 min. Levels of IL-6 and TNF-α were determined by highly sensitive enzyme-linked immunosorbent assay (ELISA) kits from R&D systems according to the manufacturer's recommendations. The absorbance was read on a microplate reader and the concentrations were calculated according to the standard curve. Protein content in the sample was determined by Commassie blue assay and the results were normalized to per microgram of protein.

4.9.   Statistical analysis

Data are expressed as means±SEM for each group. The differences among experimental groups were detected by one-way analysis of variance (ANOVA). Between groups, variance was determined using the LSD and Student–Newman–Keuls post hoc test. A p-value of less than 0.05 was considered to be statistically significant.

Acknowledgments

REFERENCES

Barrett, E.G., Johnston, C., Oberdörster, G., Finkelstein, J.N., 1999. Antioxidant treatment attenuates cytokine and chemokine levels in murine macrophages following silica exposure. Toxicol. Appl. Pharmacol. 158, 211–220.
Boekhoorn, Karin, Joels, M., Lucassen, Paul J., 2006. Increased proliferation reflects glial and vascular-associated changes, but not neurogenesis in the presenile Alzheimer hippocampus. Neurobiol. Dis. 24, 1–14.
Butterfield, D.A., Lauderback, C.M., 2002. Lipid peroxidation and protein oxidation in Alzheimer's disease brain: potential causes and consequences involving amyloid β-peptide-associated free radical oxidative stress. Free Radic. Biol. Med. 32, 1050–1060.
Buxton, G.V., Greenstock, C.L., Helman, W.P., Ross, A.B., 1998. Critical view of rate constants for reactions of hydrated electrons, hydrogen atoms and hydroxyl radicals (•OH/•OH–) in aqueous solution. J. Phys. Chem. 17, 513–886 (Ref Data).
Cai, J., Kang, Z., Liu, W.W., Luo, X., Qiang, S., Zhang, J.H., Ohta, S., Sun, X., Xu, W., Tao, H., Li, R., 2008. Hydrogen therapy reduces apoptosis in neonatal hypoxia–ischemia rat model. Neurosci. Lett. 441, 167–172.
Cai, J., Kang, Z., Liu, K., Liu, W., Li, R., Zhang, J.H., Luo, X., Sun, X., 2009. Neuroprotective effects of hydrogen saline in neonatal hypoxia–ischemia rat model. Brain Res. 1256, 129–137.
Calabrese, V., Guagliano, E., Sapienza, M., et al., 2006. Redox regulation of cellular stress response in neuron-degenerative disorders. Ital. J. Biochem. 55, 263–282.
Castellani, R.J., Harris, P.L.K., Sayre, L.M., Fujii, J., Taniguchi, N., Vitek, M.P., Founds, H., Atwood, C.S., Perry, G., Smith, M.A., 2001. Active glycation in neurofibrillary pathology of Alzheimer disease: N(epsilon)-(carboxymethyl) lysine and hexitol-lysine. Free Radic. Biol. Med. 31, 175–180.
Castranova, V., 2004. Signaling pathways controlling the production of inflammatory mediators in response to crystalline silica exposure: role of reactive oxygen/nitrogen species. Free Radic. Biol. Med. 37, 916–925.
Chapman, P.F., White, G.L., Jones, M.W., Cooper-Blacketer, D., Marshall, V.J., Irizarry, M., Younkin, L., Good, M.A., Bliss, T.V., Hyman, B.T., Younkin, S.G., Hsiao, K.K., 1999. Impaired synaptic plasticity and learning in aged amyloid precursor protein transgenic mice. Nat. Neurosci. 2, 271–276.
Chen, S.Y., Wright, J.W., Barnes, C.D., 1996. The neurochemical and behavioral effects of b-amyloid peptide (25–35). Brain Res. 720, 54–60.
Guidi, I., Galimberti, D., Lonati, S., et al., 2006. Oxidative imbalance in patients with mild cognitive impairment and Alzheimer's disease. Neurobiol. Aging 27, 262–269.
Hayashi, T., Saito, A., Okuno, S., Ferrand-Drake, M., Dodd, R.L., Nishi, T., Maier, C.M., Kinouchi, H., Chan, P.H., 2003. Oxidative damage to the endoplasmic reticulum is implicated in ischemic neuronal cell death. J. Cereb. Blood Flow Metab. 23, 1117–1128.
Huang, X., Atwood, C., Hartshorn, M.A., Multhaup, G., Goldstein, L.E., Scarpa, R.C., Cuajungco, M.P., Gray, D.N., Lim, J., Moir, R.D., Tanzi, R.E., Bush, A.I., 1999a. The A beta peptide of Alzheimer's disease directly produces hydrogen peroxide through metal ion reduction. Biochemistry 38, 7609–7616.
Huang, X., Cuajungco, M., Atwood, C.S., Hartshorn, M.A., Tyndall, J.D., Hanson, G.R., Stokes, K.C., Leopold, M., Multhaup, G., Goldstein, L.E., Scarpa, R.C., Saunders, A.J., Lim, J., Moir, R.D., Glabe, C., Bowden, E.F., Masters, C.L., Fairlie, D.P., Tanzi, R.E., Bush, A.I., 1999b. Cu(II) potentiation of Alzheimer abeta neurotoxicity. Correlation with cell-free hydrogen peroxide production and metal reduction. J. Biol. Chem. 274, 37111–37116.
Ichikawa, H., Flores, S., Kvietys, P.R., Wolf, R.E., Yoshikawa, T., Granger, D.N., Aw, T.Y., 1997. Molecular mechanisms of anoxia/reoxygenation-induced neutrophil adherence to cultured endothelial cells. Circ. Res. 81, 922–931.
Jama, J.W., Launer, L., Witteman, J.C., den Breeijen, J.H., Breteler, M.M., Grobbee, D.E., Hofman, A., 1996. Dietary antioxidants and cognitive function in a population-based sample of older persons. The Rotterdam Study. Am. J. Epidemiol. 144, 275–280.
Jiang, M.Z., Tsukahara, H., Ohshima, Y., Todoroki, Y., Hiraoka, M., Maeda, M., Mayumi, M., 2004. Effects of antioxidants and nitric oxide on TNF-alpha-induced adhesion molecule expression and NF-kappaB activation in human dermal microvascular endothelial cells. Life Sci. 75, 1159–1170.
Jiang, M.Z., Tsukahara, H., Hayakawa, K., Todoroki, Y., Tamura, S., Ohshima, Y., Hiraoka, M., Mayumi, M., 2005. Effects of antioxidants and NO on TNF-alpha-induced adhesion

molecule expression in human pulmonary microvascular endothelial cells. Respir. Med. 99, 580–591.

Keller, J.N., Schmitt, F., Scheff, S.W., Ding, Q., Chen, Q., Butterfield, D.A., et al., 2005. Evidence of increased oxidative damage in subjects with mild cognitive impairment. Neurology 64, 1152–1156.

Klafki, H.W., Staufenbiel, M., Kornhuber, J., Wiltfang, J., 2006. Therapeutic approaches to Alzheimer's disease. Brain 129, 2840–2855.

Kokura, S., Yoshida, N., Yoshikawa, T., 2002. Anoxia/reoxygenation-induced leukocyte–endothelial cell interactions. Free Radic. Biol. Med. 33, 427–432.

Koliatsos, V.E., Kecojevic, A., Troncoso, J.C., et al., 2006. Early involvement of small inhibitory cortical interneurons in Alzheimer's disease. Acta Neuropathol. (Berl.) 112, 147–162.

Lauderback, C.M., Hackett, J.M., Huang, F.F., Keller, J.N., Szweda, L.I., Markesbery, W.R., Butterfield, D.A., 2001. The glial glutamate transporter, GLT-1, is oxidatively modified by 4-hydroxy-2-nonenal in the Alzheimer's disease brain: the role of abeta1-42. J. Neurochem. 78 (2), 413–416 (Jul).

Loh, K.P., Huang, S., De Silva, R., et al., 2006. Oxidative stress: apoptosis in neuronal injury. Curr. Alzheimer Res. 3, 327–337.

Lovell, M.A., Ehmann, W.D., Mattson, M.P., Markesbery, W.R., 1997. Elevated 4-hydroxynonenal in ventricular fluid in Alzheimer's disease. Neurobiol. Aging 18, 457–461.

Markesbery, W.R., Lovell, M.A., 1998. Four-hydroxynonenal, a product of lipid peroxidation, is increased in the brain in Alzheimer's disease. Neurobiol. Aging 19, 33–36.

Mecocci, P., MacGarvey, U., Beal, M.F., 1994. Oxidative damage to mitochondrial DNA is increased in Alzheimer's disease. Ann. Neurol. 36, 747–751.

Meda, L., Baron, P., Scarlato, G., 2001. Glial activation in Alzheimer's disease: the role of abeta and its associated proteins. Neurobiol. Aging 22, 885–893.

Min, K.J., Jou, I., Joe, E., 2003. Plasminogen-induced IL-1beta and TNF-alpha production in microglia is regulated by reactive oxygen species. Biochem. Biophys. Res. Commun. 312, 969–974.

Nagele, R.G., Wegiel, J., Venkataraman, V., Imaki, H., Wang, K.C., 2004. Contribution of glial cells to the development of amyloid plaques in Alzheimer's disease. Neurobiol. Aging 25, 663–674.

Nakamura, S., Muruyama, N., Noshita, T., Annoura, H., Ohno, T., 2001. Progressive brain dysfunction following intracerebroventricular infusion of beta(1-42)-amyloid peptide. Brain Res. 912, 128–136.

Nakashima-Kamimura, N., Mori, T., Ohsawa, I., Asoh, S., Ohta, S., 2009. Molecular hydrogen alleviates nephrotoxicity induced by an anti-cancer drug cisplatin without compromising anti-tumor activity in mice. Cancer Chemother. Pharmacol. 64, 753–761.

Nunomura, A., Perry, G., Pappolla, M.A., Wade, R., Hirai, K., Chiba, S., Smith, M.A., 1999. RNA oxidation is a prominent feature of vulnerable neurons in Alzheimer's disease. J. Neurosci. 19, 1959–1964.

Nunomura, A., Perry, G., Aliev, G., Hirai, K., Takeda, A., Balraj, E.K., Jones, P.K., Ghanbari, H., Wataya, T., Shimohama, S., Chiba, S., Atwood, C.S., Petersen, R.B., Smith, M.A., 2001. Oxidative

damage is the earliest event in Alzheimer disease. J. Neuropathol. Exp. Neurol. 60, 759–767.

Ohsawa, I., Ishikawa, M., Takahashi, K., Watanabe, M., Nishimaki, K., Yamagata, K., Katsura, K., Katayama, Y., Asoh, S., Ohta, S., 2007. Hydrogen acts as a therapeutic antioxidant by selectively reducing cytotoxic oxygen radicals. Nat. Med. 13, 688–694.

Ohsawa, I., Nishimaki, K., Yamagata, K., Ishikawa, M., Ohta, S., 2008. Consumption of hydrogen water prevents atherosclerosis in apolipoprotein E knockout mice. Biochem. Biophys. Res. Commun. 377, 1195–1198.

Ohta, S., Ohsawa, I., 2006. Dysfunction of mitochondria and oxidative stress in the pathogenesis of Alzheimer's disease: on defects in the cytochrome coxidase complex and aldehyde detoxification. J. Alzheimers Dis. 9, 155–166.

Perrig, W.J., Perrig, P., Stähelin, H.B., 1997. The relation between antioxidants and memory performance in the old and very old. J. Am. Geriatr. Soc. 445, 718–724.

Picklo, M.J., Olson, S.J., Markesbery, W.R., Montine, T.J., 2001. Expression and activities of aldo-keto oxidoreductases in Alzheimer disease. J. Neuropathol. Exp. Neurol. 60 (7), 686–695 (Jul).

Prediger, R.D., Franco, J.L., Pandolfo, P., Medeiros, R., Duarte, F.S., Di Giunta, G., Figueiredo, C.P., Farina, M., Calixto, J.B., Takahashi, R.N., Dafre, A.L., 2007. Differential susceptibility following beta-amyloid peptide-(1-40) administration in C57BL/6 and Swiss albino mice: evidence for a dissociation between cognitive deficits and the glutathione system response. Behav. Brain Res. 27, 205–213.

Rottkamp, C.A., Nunomura, A., Hirai, K., Sayre, L.M., Perry, G., Smith, M.A., 2000. Will antioxidants fulfill their expectations for the treatment of Alzheimer disease? Mech. Ageing Dev. 116, 169–179.

Sayre, L.M., Zelasko, D.A., Harris, P.L., Perry, G., Salomon, R.G., Smith, M.A., 1997. 4-Hydroxynonenal-derived advanced lipid peroxidation end products are increased in Alzheimer's disease. J. Neurochem. 68, 2092–2097.

Shah, R.S., Lee, H-G., Xiongwei, Z., Perry, G., Smith, M.A., Castellani, R.J., 2008. Current approaches in the treatment of Alzheimer's disease. Biomed. Pharmacother. 62, 199–207.

Shen, Y.X., Xu, S.-Y., Wei, W., Wang, X.L., Sun, X., 2002. Melatonin blocks rat hippocampal neuronal apoptosis induced by amyloid beta-peptide 25–35. J. Pineal Res. 32, 163–167.

Smith, W.W., Gorospe, M., Kusiak, J.W., 2006. Signaling mechanisms underlying abeta toxicity: potential therapeutic targets for Alzheimer's disease. CNS Neurol. Disord. Drug Targets 5, 355–361.

Walsh, D.M., Klyubin, I., Fadeeva, J.V., Cullen, W.K., Anwyl, R., Wolfe, M.S., Rowan, M.J., Selkoe, D.J., 2002. Naturally secreted oligomers of amyloid beta protein potently inhibit hippocampal long-term potentiation in vivo. Nature 416, 535–539.

Weiner, H.L., Selkoe, D., 2002. Inflammation and therapeutic vaccination in CNS diseases. Nature 420, 879–884.

Zhu, X., Lee, H.G., Moreira, P.I., et al., 2006. Presenilin mutation: a deadly first hit in Alzheimer disease. A commentary on "Aging sensitizes towards ROS formation and lipid peroxidation in PS1M146L transgenic mice". Free Radic. Biol. Med. 40, 737–739.